Journal of Catalysis 281 (2011) 119–127

Contents lists available at ScienceDirect

Journal of Catalysis

journal homepage: www.elsevier.com/locate/jcat

Influence of activated carbon surface chemistry on the activity of Au/AC catalysts in glycerol oxidation

Elodie G. Rodrigues [a], Manuel F.R. Pereira [a], Xiaowei Chen [b], Juan J. Delgado [b], José J.M. Órfão [a,*]

[a] *Laboratório de Catálise e Materiais (LCM), Laboratório Associado LSRE/LCM, Departamento de Engenharia Química, Faculdade de Engenharia, Universidade do Porto, Rua Dr. Roberto Frias, 4200-465 Porto, Portugal*

[b] *Departamento de Ciência de los Materiales e Ingeniería Metalúrgica y Química Inorgánica, Facultad de Ciencias, Universidade de Cadiz, Campus Rio San Pedro, 11510 Puerto Real, Cadiz, Spain*

ARTICLE INFO

Article history:
Received 2 February 2011
Revised 29 March 2011
Accepted 13 April 2011
Available online 17 May 2011

Keywords:
Glycerol
Oxidation
Gold
Activated carbon
Surface chemistry
Mechanism

ABSTRACT

The main goal of this work is the study of the relationship between the surface chemical characteristics of activated carbon and the performance of the respective gold-supported catalysts in the oxidation of glycerol. For that purpose, a set of modified activated carbons with different levels of oxygenated functional groups on the surface, but with no major differences in their textural parameters, was prepared. A strong effect of the activated carbon surface chemistry on the catalytic activity was observed. Gold particles with similar average sizes resulted in different performances, being the surface oxygenated acid groups particularly prejudicial for the catalytic activity. Basic oxygen-free supports characterized by a high density of free π-electrons lead to more active catalysts; the observation was tentatively explained on the basis of a recent proposed mechanism by considering the capability to promote electron mobility. However, the presence of oxygenated groups on the support does not influence significantly the selectivities.

1. Introduction

Over the last decades, biodiesel has emerged as a viable clean fuel. During its production via transterification of oils from plants, about 100 kg of glycerol is produced for every ton of biodiesel [1]. During the last years, this market has been continuously increasing, and it is expected that this trend remains [1]. The rapid expansion of the global production of biodiesel has created a major surplus of glycerol, leading to a decline in glycerin pricing. Consumption of this extra glycerol is a necessary requisite for the commercial viability of biodiesel production. Liquid phase catalytic oxidation is a promising route to the valorization of glycerol by its conversion into useful compounds, provided that catalysts used are sufficiently active and selective for the formation of compounds such as glyceric acid (GLYCEA) and/or dihydroxyacetone (DIHA), potentially useful as chemical intermediates in the fine chemicals industry, particularly in pharmaceuticals [1,2]. However, the extensive functionalization of the glycerol molecule, with similar reactive hydroxyl groups, renders its selective oxidation particularly difficult [3,4].

Recently, there have been many studies dealing with the oxidation of glycerol to chemical intermediates using supported gold nanoparticles as catalysts [5–7]. One of the advantages of using this metal is related with its strong resistance to oxygen poisoning, compared with platinum-based catalysts, allowing for the use of high oxygen partial pressures [8]. However, under alkaline conditions, catalyst performance and selectivity seem to mainly depend on the nanoparticles size, which in turn can be controlled by the preparation method [9,10]. Generally, small nanoparticles (5 nm) were found to be more active than larger particles (20 nm) [11]. Apparently, the gold–sol immobilization method is the most appropriate technique in order to obtain these well-dispersed nanoparticles on carbons [9,12]. In addition to the particles size, the activity of gold catalysts seems to be affected by the nature of support. Nano-sized gold particles supported on different carbon materials (e.g., carbon black, activated carbon, and graphite) and oxides (TiO_2, MgO, and Al_2O_3) are active for the oxidation of glycerol but show very different performances, being carbon-supported gold catalysts more active than most oxides-supported catalysts [5,8,13]. However, even when different carbon materials are compared, textural and chemical properties could largely differ, which make the role of the support complex to understand. Moreover, in spite of its well-known influence on the catalyst activity, the role of the support in the mechanism of glycerol oxidation is still not clear.

---

* Corresponding author. Fax: +351 225 081 449.
E-mail addresses: elodie.rodrigues@fe.up.pt (E.G. Rodrigues), fpereira@fe.up.pt (M.F.R. Pereira), xiaowei.chen@uca.es (X. Chen), juanjose.delgado@uca.es (J.J. Delgado), jjmo@fe.up.pt (J.J.M. Órfão).

0021-9517/$ - see front matter © 2011 Elsevier Inc. All rights reserved.
doi:10.1016/j.jcat.2011.04.008

In this study, a NORIT ROX 0.8 activated carbon was modified by chemical and thermal treatments in order to obtain supports with different surface chemical properties, but with no major differences in their textural parameters. The sol immobilization method was used for preparing gold catalysts supported on the different activated carbon samples. Then, the performance of the prepared catalysts was investigated and the possible role of the support surface chemistry in the reaction mechanism was discussed.

2. Experimental

2.1. Materials and methods

2.1.1. Materials

The gold precursor, $HAuCl_4.3H_2O$ (99.99% ACS, Au 49.5% min), was supplied by Alfa Aesar. $NaBH_4$ of purity >95% from Riedel-de-Haël, NaOH (>97%) and polyvinylalcohol (PVA) (purity >99%) from Aldrich were used. The commercial activated carbon NORIT ROX 0.8 was selected as starting material for the preparation of supports.

2.1.2. Preparation procedures

The NORIT ROX 0.8 activated carbon has a small amount of surface oxygenated groups. In order to evaluate how catalyst activity correlates with the concentration of those groups, the original support was modified by chemical and thermal treatments in order to obtain supports with different surface chemical properties. Gold was supported on these modified activated carbon materials by the sol immobilization method.

2.1.2.1. Preparation of modified activated carbons. A NORIT ROX 0.8 activated carbon (pellets of 0.8 mm diameter and 5 mm length) was used as starting material for this study (sample AC_0). This sample was submitted to different chemical and thermal treatments in order to obtain materials with different surface chemistries, while maintaining the original textural properties as far as possible.

2.1.2.1.1. Oxidation treatment. Initially, HNO_3 6 M was introduced into a round-bottom flask. A Soxhlet extraction apparatus with activated carbon AC_0 was connected to the flask and to a condenser. The acid solution was heated to boiling temperature, and the reflux was stopped after 3 h. The oxidized material was subsequently washed with distilled water until neutral pH, and then dried at 110 °C for 24 h (sample AC_1). The purpose of this liquid-phase oxidation is to increase the amount of oxygen-containing surface groups on the support.

2.1.2.1.2. Thermal treatments. Sample AC_1 was used as the starting material for the thermal treatments since it is important that the starting material presents a large amount of surface groups in order to produce activated carbons with a highly basic character [14]. Support AC_1 was treated under nitrogen flow for 30 min at different temperatures (400, 600, or 900 °C) followed by a treatment under dry air flow at room temperature for 1 h. Therefore, the following samples were prepared: AC_{1tt400}, AC_{1tt600}, AC_{1tt900}. The same procedure was repeated but under a flow of hydrogen at 900 °C (sample $AC_{1tt900\text{-}H2}$).

These thermal treatments selectively remove the oxygen-containing surface groups, previously introduced in the treatment with HNO_3, by thermal degradation [15,16]. The final treatment under air is intended to stabilize the surface chemistry of the samples. Besides, thermal treatments under H_2 flow are expected to generate higher basicity on the surface of the carbon than thermal treatments under N_2 flow [17].

After these treatments, all samples were ground to a particle diameter between 0.1 and 0.3 mm before use.

2.1.2.2. Preparation of catalysts. Gold on carbon catalysts were prepared by the sol immobilization method with $NaBH_4$ as reducing agent [18]. Briefly, $HAuCl_4{\cdot}3H_2O$ (35.1 mg) was dissolved in 690 mL of H_2O, and polyvinyl alcohol was added (1.6 mL, 0.2 wt%) under stirring. The gold colloid was subsequently reduced by the addition of $NaBH_4$ (4 mL, 0.1 M) under vigorous magnetic stirring. The resulting ruby-red sol was formed immediately. Within a few minutes of sol generation, the colloid was immobilized by adding the support under vigorous stirring. The amount of support was calculated to reach a final nominal metal loading of 1 wt%. After 3–4 days, the colorless solution was filtered, the catalyst washed thoroughly with distilled water until the filtrate was free of chloride ($AgNO_3$ test) and dried at 110 °C for 24 h. After heat treatment under N_2 flow for 3 h at 350 °C, in order to remove any possible organic waste, the catalysts were activated by reduction in a stream of H_2 flow for 3 h at 350 °C.

2.2. Characterization

The supports were characterized by N_2 adsorption at −196 °C in a NOVA Quantachrome Instruments apparatus.

The qualitative and quantitative determination of oxygenated surface functional groups was performed by temperature programmed desorption – mass spectrometry (TPD-MS) [15,16]. CO and CO_2 TPD spectra were obtained with a fully automated AMI-200 equipment (Altamira Instruments). The samples (150 mg) were placed in a U-shaped quartz tube inside an electrical furnace and subjected to a 5 °C min^{-1} linear temperature increase up to 1100 °C under helium flow (25 $Ncm^3\ min^{-1}$). A quadrupole mass spectrometer (Dymaxion 200, Ametek) was used to monitor CO and CO_2 signals. For quantification of the CO and CO_2 released, calibration of these gases was carried out at the end of each analysis.

In some cases, the determination of the pH at the point of zero charge (pH_{pzc}) was also carried out.

The average metal particles size was determined by high-resolution transmission electron microscopy (HRTEM) using a JEOL2010F instrument, with 0.19 nm spatial resolution at Scherzer defocus conditions. High Angel Annular Dark Field – Scanning Transmission Electron Microscopy (HAADF-STEM) images were obtained with the same microscope. The average diameter was calculated by the measurement of at least 200 particles.

The noble metal loading of the samples was determined by inductively coupled plasma (ICP) analysis using an Iris Intrepid Spectrometer (Thermo Elemental). An Ethos 1600 microwave labstation (Milestone) was used to prepare the acid solution of all the samples for ICP analysis.

Details of these characterization methods are described elsewhere [19].

2.3. Catalysts evaluation

The standard oxidation experiments were carried out with oxygen under 3 bar, at 60 °C. NaOH solution (NaOH/glycerol molar ratio = 2) and catalyst (700 mg) were added to a 0.3 M aqueous solution of glycerol (V = 150 mL) under stirring at 1000 rpm. Additionally, a limited number of runs were carried out at different oxygen pressures (6, 10 bar) or temperatures (40, 80 °C). After heating under nitrogen to the selected temperature, the reaction was initiated by switching from inert gas to oxygen.

The reaction was monitored by taking samples (0.5 mL) for analysis at regular time intervals. The quantitative analysis of mixtures was carried out by high-performance liquid chromatography (HPLC). The chromatograph (Elite LaChrom HITACHI) was equipped with a refractive index and an ultraviolet (210 nm) detector. Reactant and products were separated on an ion exclusion column (Alltech OA 1000). Products were identified by comparison with standard samples. Glycerol (>99.5%) was purchased from Fluka, glyceric acid (GLYCEA), dihydroxyacetone (DIHA) and the by-products glycolic acid (GLYCOA), glyceraldehyde (GLYCER), tartronic acid (TARTA), and oxalic acid (OXALA) were obtained from Sigma–Aldrich. Further details can be found elsewhere [19]. The selectivities (S_i) into the different products i at time t were calculated as:

$$S_i = \frac{C_i}{\nu_i \cdot C_0 \cdot X} \tag{1}$$

where C_i is the concentration of product i (mol L^{-1}), C_0 is the initial concentration of glycerol (mol L^{-1}), X is the glycerol conversion, and ν_i corresponds to the moles of i produced per mol of glycerol consumed, according to the stoichiometry.

3. Results and discussion

3.1. Characterization of supports and catalysts

The main goal of the present work is to study the relationship between the surface chemical characteristics of activated carbons and the catalytic performance of gold supported on these materials for glycerol oxidation. For that purpose, a set of modified activated carbons with different levels of acidity/basicity was prepared. Both liquid-phase oxidations and thermal treatments have been reported not to significantly change the textural properties of activated carbons [15,16].

3.1.1. Textural properties

The textural characterization of the different supports and of the Au/AC$_0$ catalyst is presented in Table 1. As expected, no drastic changes in the textural properties of the materials were observed. The slight decrease in AC$_1$ surface area may be due to the abundant presence of oxygen-containing groups introduced on the surface of the activated carbon by the treatment with HNO$_3$, which possibly block the entry of N$_2$ inside the small pores, as reported by Yin et al. [20]. After treatment at 900 °C, the mentioned functional groups were removed by thermal decomposition and the area of the corresponding support slightly increased comparatively to the original carbon [21].

The BET surface area of the Au/AC$_0$ catalyst decreased only slightly compared with the unloaded carbon. Therefore, it was assumed that the textural properties of modified supports and supported gold catalysts are not significantly different from those of the original activated carbon.

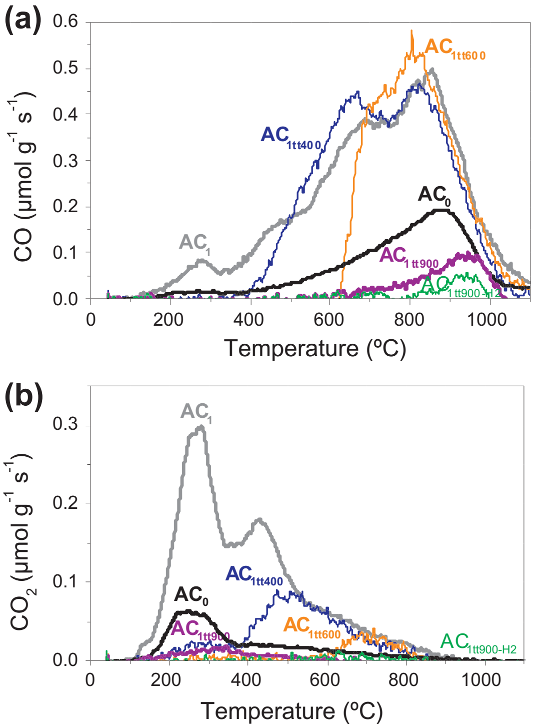

Fig. 1. TPD spectra of the different activated carbons: (a) CO; (b) CO$_2$.

3.1.2. Surface chemistry characterization

TPD is a thermal analysis method that is becoming popular for the characterization of the oxygen-containing groups on the surface of carbon materials. In this technique, the total amount of the various oxygenated surface groups (carboxylic acids, carboxylic anhydrides, lactones, phenols, and carbonyls or quinones) on carbon materials can be determined, since these groups are decomposed upon heating by releasing CO and/or CO$_2$ at different temperature ranges. Accordingly, it is possible to identify and estimate the amount of the oxygenated groups on a given material by TPD experiments. The nature of the groups can be assessed by the decomposition temperature and the type of gas released, and their respective amounts determined by the areas of the component peaks, obtained by deconvolution techniques [15,16]. It was reported that CO$_2$ results from the decomposition of carboxylic acids at low temperatures (150–450 °C) or from lactones at high temperatures (600–800 °C); carboxylic anhydrides originate both CO and CO$_2$ (400–650 °C); groups such as phenols (600–800 °C), and carbonyls and quinones (750–1000 °C) originate CO [15,16]. Consequently, an increase in the amount of surface oxygen is evidenced by the increase in CO and CO$_2$ released.

Table 1
Textural properties and pHpzc of activated carbons and the Au/AC$_0$ catalyst.

Sample	S_{BET} (m^2/g)	S_{meso} (m^2/g)	V_{micro} (cm^3/g)	pHpzc
AC$_0$	1025	180	0.361	7.9
AC$_1$	965	156	0.369	3.2
AC$_{1tt400}$	952	200	0.350	–
AC$_{1tt600}$	1042	150	0.391	–
AC$_{1tt900}$	1106	184	0.399	8.2
AC$_{1tt900-H2}$	1062	193	0.359	9.0
Au/AC$_0$	958	195	0.343	–

Fig. 1a and b shows, respectively, the CO and CO$_2$ TPD spectra of the commercial activated carbon as received (AC$_0$) and the modified samples. The deconvolution of these CO and CO$_2$ spectra was carried out in order to determine the amount of each surface group. A multiple Gaussian function was used for fitting each spectrum. The numerical calculations were based on a non-linear routine, which minimized the sum of squared deviations, using the Levenberg–Marquardt method to perform the iterations and some assumptions according to [15,16]. Table 2 shows the results obtained.

Analyzing the results, it is clear that the sample AC$_1$, which was oxidized with HNO$_3$, has the highest amount of oxygen-containing surface groups. The liquid-phase oxidation significantly increased the amount of CO$_2$ evolved at low temperatures (carboxylic acid groups) and CO at high temperatures (phenol and carbonyl/quinone groups). As a result, the oxidized sample AC$_1$ has a low pH$_{pzc}$ (see Table 1) due to the introduction of the mentioned oxygen-containing functional groups with acidic properties, namely carboxylic acids (see Table 2), originating a support with acidic and hydrophilic characteristics [22]. Thermal treatments selectively remove the oxygen-containing surface groups, originating materials with progressively lower oxygen contents (see Fig. 1 and Table 2). It can also be observed in Table 2 that the amount of carboxylic acids

Table 2
Amounts of the different oxygenated surface groups present on activated carbon supports (obtained by deconvolution of CO_2 and CO spectra) and total amounts of CO, CO_2 and oxygen released.

Sample	Carboxylic acids (μmol g^{-1})	Carboxylic anhydrides (μmol g^{-1})	Lactones (μmol g^{-1})	Phenols (μmol g^{-1})	Carbonyl /quinones (μmol g^{-1})	CO (μmol g^{-1})	CO_2 (μmol g^{-1})	O (μmol g^{-1})
AC_0	134	37	18	191	500	776[a]	189	1154
AC_1	608	239	82	788	1209	2414[a]	929	4272
AC_{1tt400}	48	233	75	895	1082	2210	356	2922
AC_{1tt600}	44	27	101	658	1080	1765	172	2109
AC_{1tt900}	84	31	12	71	170	272	127	526
$AC_{1tt900\text{-}H2}$	0	0	0	26	70	96	0	96

[a] The total amount of CO is slightly higher than the sum of the groups that decompose releasing CO. The justification can be found elsewhere [16].

and anhydrides considerably decreases for thermal treatments above 400 °C; on the other hand, phenols and carbonyl/quinones only decrease significantly after heat treatment above 600 °C. As can be seen in the TPD spectra of samples AC_{1tt900} and $AC_{1tt900\text{-}H2}$, the CO_2 and CO releasing groups have almost completely been removed; these samples have basic properties [17]. According to Leon y Leon et al. [23], this basic character is mainly due to the electron rich oxygen-free sites located on the carbon basal planes. It was also reported that heat treatments under hydrogen flow at high temperatures are more effective in removing oxygen than under inert atmosphere, once they originate stable basic surfaces by forming stable C–H bonds, whereas the activated carbon heat treated under nitrogen has a surface with reactive sites capable of readsorbing oxygen, leading to the formation of some of the previously removed groups, as it can be observed in Table 2 [17]. This is in agreement with our TPD data, since sample AC_{1tt900} shows a higher content of CO_2 releasing groups than sample $AC_{1tt900\text{-}H2}$ (see Fig. 1 and Table 2). As expected, sample $AC_{1tt900\text{-}H2}$ has the highest pH_{pzc} value (see Table 1) and corresponds to the most basic material.

3.1.3. Microscopy and ICP analyses

HAADF-STEM images were collected in order to get information about metal particle size distributions (Fig. 2). The average crystallite sizes of the studied catalysts are presented in Table 3. For oxidation catalysis by gold, it has been shown that the average particle size influences both activities and selectivities [9,24]. Although small gold particle sizes (<5 nm) have a higher activity, catalysts with gold crystallites as large as 42 nm have already shown a relevant activity in glycerol oxidation [24]. Carrettin et al. [25] reported that active catalytic sites have a broad size distribution between 15 and 30 nm diameter for gold nanoparticles supported on carbon, the 15 nm size being predominant.

Nevertheless, in the present work, gold catalysts prepared by the sol immobilization method have particles with sizes lower than 15 nm, and therefore, these catalysts are expected to be highly active. The same impregnation procedure was used in order to obtain gold catalysts with similar particle sizes, independently of the support used. This was effectively achieved for $Au/AC_{0,}$ Au/AC_{1tt400}, Au/AC_{1tt600}, Au/AC_{1tt900}, and $Au/AC_{1tt900\text{-}H2,}$ which have fairly low and similar average gold particle sizes, suggesting that the difference in the performance of these catalysts will be mainly due to the different chemical surface properties of the supports. The Au/AC_1 sample has a higher average particle size. This can be due to the large amount of oxygen-containing groups on support AC_1, which could influence the metal dispersion. On one hand, the surface oxygenated groups are considered to act as anchoring sites that interact with metallic precursors, improving the metal dispersion [26]. However, some of these functional groups present on activated carbon are easily decomposed upon heating even at low temperatures. This occurs with some carboxylic acid groups, which already decompose at temperatures below 350 °C, as it can be seen in the TPD spectra (Fig. 1). The sample AC_1 is the unique support that has a significant amount of oxygenated groups able to decompose at temperatures below 350 °C (Fig. 1). Therefore, during the heat treatment and reducing steps used in the preparation of the Au/AC_1 catalyst, some groups are thermally decomposed and the gold particles that are anchored to them may have a low stability and could be prone to sintering. This can possibly explain why the Au/AC_1 catalyst has larger metallic particles than Au/AC_0, Au/AC_{1tt400}, Au/AC_{1tt600}, Au/AC_{1tt900}, and $Au/AC_{1tt900\text{-}H2}$, because on this latter group of samples, contrarily to the former, there was no oxygenated groups that decompose at low temperatures during the preparation step. The supports AC_{1tt400}, AC_{1tt600}, AC_{1tt900}, and $AC_{1tt900\text{-}H2}$ were already heat treated at temperatures above 350 °C before gold impregnation; therefore, as it can be seen in TPD spectra (Fig. 1), they do not release CO and/or CO_2 below 350 °C.

Table 3 summarizes the metal loadings of the catalysts. The gold content obtained by ICP analysis is slightly lower than the nominal. However, chemical and heat treatments of activated carbon did not influence substantially the gold content of catalysts and all the samples present a similar value of approximately 0.6%.

3.2. Kinetic experiments

3.2.1. Influence of pressure and temperature

The influence of oxygen pressure and temperature on the reaction was examined for the Au/AC_0 catalyst. Experiments were carried out with 150 mL of glycerol (0.3 M), NaOH/glycerol = 2 mol/mol, and 700 mg of catalyst. The oxygen pressure was varied between 3 and 10 bar and the temperature between 40 and 80 °C.

Under the tested conditions, it was found that the reaction rate increases with the oxygen pressure as depicted in Fig. 3a). For instance, when this value is 10 bar, total glycerol conversion is achieved after about 1.5 h. Moreover, selectivity to DIHA slightly increases with the increase in oxygen pressure, while selectivity to unwanted GLYCOA decreases (Table 4).

The temperature increase also leads to an increase in the catalytic activity as seen in Fig. 3b), but appears to be very unfavorable for the selectivity to the products of interest, especially for glyceric acid, which seems to oxidize very easily to glycolic acid at high temperatures (Table 4). This result was described before by Porta and Prati [9] under similar conditions.

For comparative purposes, selectivities to the different products are presented at constant reaction time (2 h) and also at the same glycerol conversion (90%) in Table 4. The selectivities obtained are practically independent of time and glycerol conversion, varying only slightly during the reaction for all the conditions and catalysts tested in this work. As an illustrative example, the evolution of DIHA and GLYCEA selectivities as a function of glycerol conversion in the presence of Au/AC_0 at different oxygen pressures and reaction temperatures can be seen in Fig. 3c and d, respectively. In some cases, the sum of the calculated selectivities is lower than

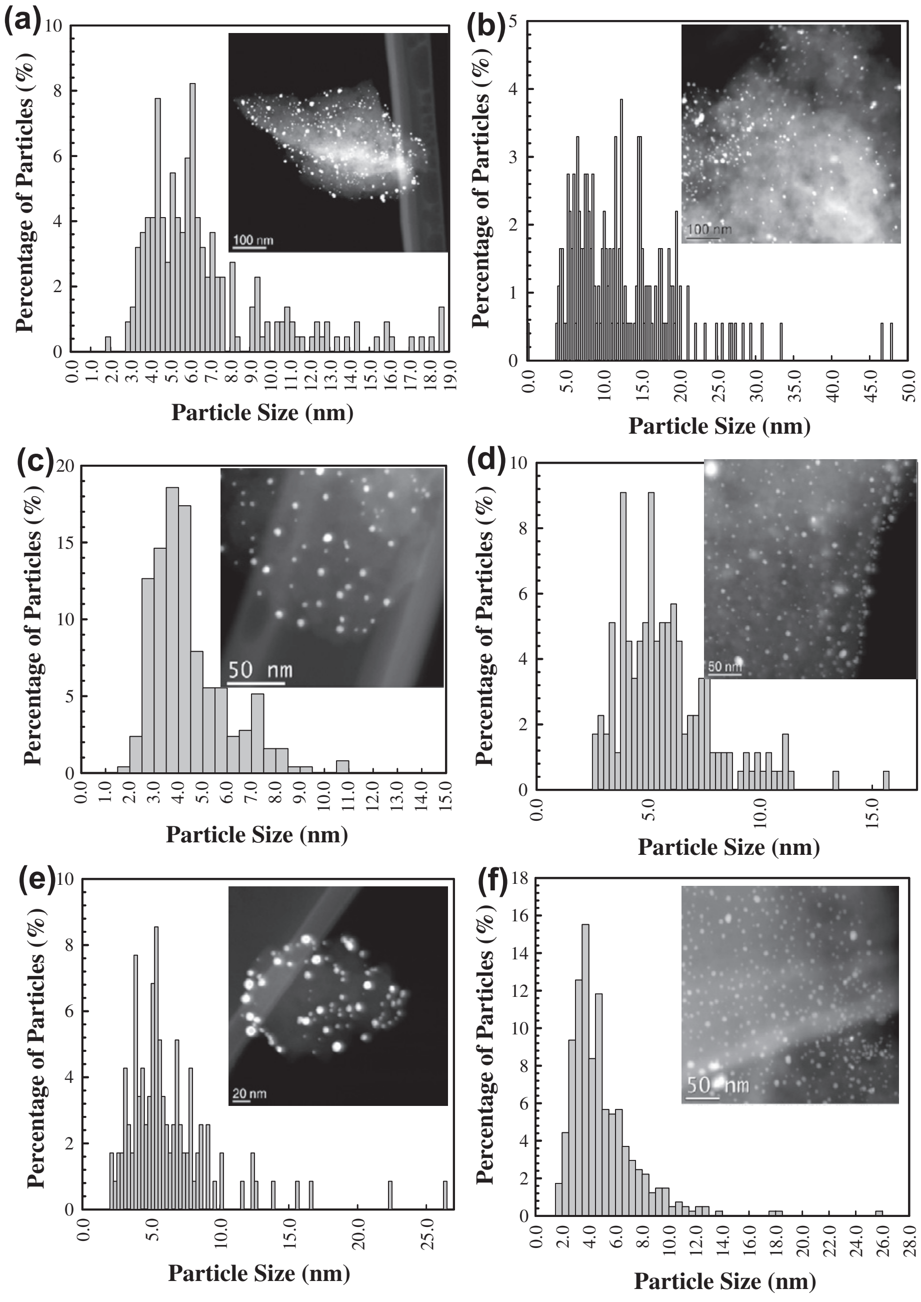

Fig. 2. Particle size distributions and HAADF-STEM images of the Au catalysts supported on (a) AC_0, (b) AC_1, (c) AC_{1tt400}, (d) AC_{1tt600}, (e) AC_{1tt900}, and (f) $AC_{1tt900\text{-}H2}$.

Table 3
Average crystallite size and metal content of the studied catalysts.

Catalyst	Loading (wt%)[a]	d_M (nm)
Au/AC_0	0.59	6.8
Au/AC_1	0.62	12.5
Au/AC_{1tt400}	0.60	4.4
Au/AC_{1tt600}	0.56	5.8
Au/AC_{1tt900}	0.57	6.4
$Au/AC_{1tt900\text{-}H2}$	0.66	5.0
Au/AC_0 (after 2 run)	0.62	8.3
Au/AC_0 (after 4 run)	0.56	11.4

[a] Obtained by ICP analysis after combustion of activated carbon.

1 (see Table 4), since some oxalic acid was also detected but always with low concentrations.

It should be noticed that the comparison between the results obtained in this work and those reported in literature is particularly difficult since the reaction conditions changed from author to author. Moreover, the results are often presented as conversion obtained after a certain reaction time. For example, under conditions identical to the present research, Carretin et al. [27] obtained 56% glycerol conversion after 3 h of reaction at 60 °C and 3 bar using 1 wt% Au/graphite. In the present work, total conversion was achieved at this same reaction time with Au/AC_0. Additionally, the turnover frequencies (TOFs) calculated after 1 h of reaction for the Au/AC_0 catalyst tested at different temperatures, and oxygen pressures are shown in Table 5 and compared with some typical results from the literature [28–30]. It can be concluded that the activities obtained in this work are similar or even higher than those reported by different groups.

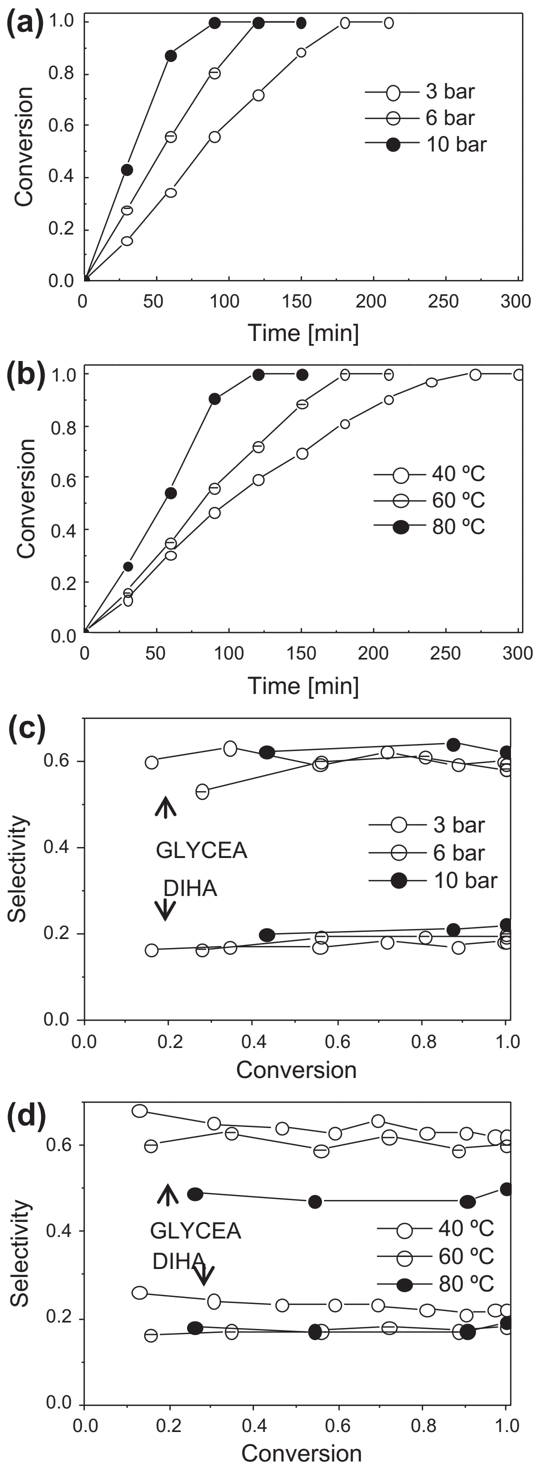

Fig. 3. Glycerol conversion over Au/AC$_0$ varying (a) the oxygen pressure or (b) the temperature, and evolution of DIHA and GLYCEA selectivities as a function of glycerol conversion at different (c) oxygen pressures and (d) reaction temperatures. Reaction conditions: 150 mL of glycerol 0.3 M, catalyst amount = 700 mg, NaOH/glycerol = 2 mol/mol.

It is important to mention that about 85% total selectivity to products of commercial interest was achieved at 40 °C and 3 bar or 60 °C and 10 bar. Then, it may be concluded that gold prepared by the sol immobilization method is highly effective, and the selectivity can be slightly altered by changing the reaction conditions. Furthermore, gold allows high levels of oxygen in the reaction medium without suffering any significant deactivation.

3.2.2. Investigation of the support effects in the glycerol oxidation

Fig. 4 shows the evolution of glycerol conversion in the presence of the gold catalysts prepared on different activated carbons. The surface chemical functional groups of activated carbon can be controlled by chemical and heat treatments. Since no drastic changes were observed in the textural properties of the supports (cf. Table 1), in gold average particle sizes and in metal loadings of the catalysts (cf. Table 3), the disparities in performances observed in Fig. 4 must be related almost exclusively to the differences in support chemical properties. In fact, whether the activity was only dependent on the gold particles size, the following order of performances would be expected: Au/AC$_{1tt400}$ > Au/AC$_{1tt900\text{-}H2}$ > Au/AC$_{1tt600}$ > Au/AC$_{1tt900}$ > Au/AC$_0$ > Au/AC$_1$ (see Table 3). However, sample Au/AC$_{1tt400}$, which has the smallest gold particles size (average diameter = 4.4 nm), only shows a weak efficiency in glycerol oxidation, mainly when compared with Au/AC$_{1tt900\text{-}H2}$, which has a similar average particle size (5.0 nm), but also with Au/AC$_0$ (6.8 nm) and Au/AC$_{1tt900}$ (6.4 nm). These catalysts, all with similar distributions of gold particle sizes, clearly resulted in different performances depending on the amount of oxygenated groups on the carbon surface. In general, as the oxygenated groups of the support are removed, the catalytic performance gradually increases.

We also tested the Au/AC$_0$ catalyst in successive experiments. Each run was carried out under the standard conditions described previously. The catalyst was recovered by filtering off the solution of the previous run after 5 h of reaction and reused. Due to some losses during the filtration procedure, a limited amount of fresh catalyst (<5% of the total weight) was also added to the reaction medium. It can be observed in Fig. 5 that the first two runs correspond to similar results, but in the third and mainly in the fourth the catalyst performance significantly decreased (conversion after 2 h is about 40% lower in run 4). ICP analyses (see Table 3) show that the gold content remains unchanged after the four runs; then, metal leaching is not the cause of the observed deactivation. However, a growing size of Au particles was observed by microscopy analysis of the recovered catalyst after successive experiments (see Table 3), which probably explains the poor performance. On the other hand, this may affect positively the selectivity to GLYCEA, which slightly increased from 0.62 on the first run to 0.65 on the fourth, whereas the selectivity to DIHA remains practically unchanged (Fig. 5). The effect of the particle size on the GLYCEA selectivity is in agreement with the results of Porta and Prati [9]. Although these authors [9] prepared gold catalysts by a similar PVA-protected sol preparation, they used them directly as obtained after the synthesis (i.e., without any previous heat treatments in N_2 and H_2, as described in Section 2.1.2.2). In order to study the influence of the mentioned activation in the catalyst performance, we tested the Au/AC$_0$ catalyst as obtained and heat treated at 350 °C. A better performance was achieved with the catalyst prepared by the standard procedure (Section 2.1.2.2), as it can be seen in Table 5 (TOF reduces by more than 50% in the catalyst prepared without heat treatments). Moreover, successive runs carried out under the standard experimental conditions with the Au/AC$_0$ catalyst, with or without heat treatments at 350 °C (data not shown), allow to conclude that deactivation of the catalyst used without heat treatments is much more significant than that of the sample heat treated at 350 °C. For example, the glycerol conversion after 2 h in the third run is about 25% lower in the presence of the catalyst prepared by the standard procedure (Fig. 5), while the sample used without PVA removal leads to a relative conversion decrease of 53%. Moreover, it was observed by microscopy analysis of the recovered catalyst after successive experiments that the average size of gold particles in the sample Au/AC$_0$ heat treated at 350 °C increases from 6.8 nm (fresh catalyst) to 11.4 nm after four runs (see Table 3), while the average crystallite size of the sample used

Table 4
GLYCEA, GLYCOA, DIHA, and TARTA selectivities (S_{GLYCEA}, S_{GLYCOA}, S_{DIHA}, S_{TARTA}) at different oxygen pressures and temperatures for 90% glycerol conversion (X_{GLY}) and after 2 h of reaction with the Au/AC$_0$ catalyst.

Catalyst	t = 120 min					X_{GLY} = 90%			
	X_{GLY}	S_{GLYCEA}	S_{GLYCOA}	S_{DIHA}	S_{TARTA}	S_{GLYCEA}	S_{GLYCOA}	S_{DIHA}	S_{TARTA}
Au/AC$_0$									
3 bar[a]	0.72	0.62	0.15	0.18	0.05	0.59	0.14	0.17	0.05
6 bar[a]	1	0.60	0.10	0.19	0.05	0.61	0.11	0.19	0.05
10 bar[a]	1	0.63	0.10	0.22	0.05	0.64	0.10	0.21	0.05
40 °C[b]	0.59	0.62	0.11	0.22	0.05	0.63	0.10	0.21	0.06
60 °C[b]	0.72	0.62	0.15	0.18	0.05	0.59	0.14	0.17	0.05
80 °C[b]	1	0.50	0.26	0.19	0.05	0.47	0.25	0.17	0.05

[a] Reaction conditions: 60 °C, 150 mL of glycerol 0.3 M, NaOH/glycerol = 2 mol/mol, catalyst amount = 700 mg.
[b] Reaction conditions: p_{O_2} = 3 bar, 150 mL of glycerol 0.3 M, NaOH/glycerol = 2 mol/mol, catalyst amount = 700 mg.

Table 5
Comparison between turnover frequencies (TOFs) obtained after 1 h of reaction for the Au/AC$_0$ catalyst tested at different temperatures and oxygen pressures and some typical results from the literature.

Reaction conditions			TOF (h^{-1})	Ref.
T (°C)	p_{O_2} (bar)	NaOH/GLY (mol/mol)		
40	3	2	3930	This work
60	3	2	4050	This work
60	3	2	1800[a]	This work
60	6	2	6550	This work
60	10	2	10,080	This work
80	3	2	7070	This work
60	10	2	8640	[28]
50	3	4	900	[29]
50	3	4	830	[30]
70	3	4	960	[30]

[a] Au/AC$_0$ catalyst used without prior heat treatments at 350 °C.

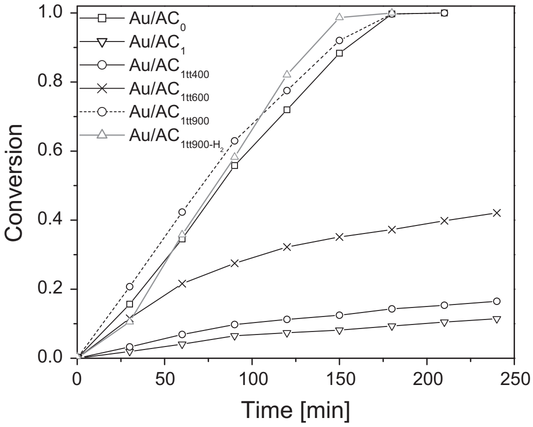

Fig. 4. Influence of the modified activated carbon supports on the performance of gold catalysts. Reaction conditions: 60 °C, p_{O_2} = 3 bar, 150 mL of glycerol 0.3 M, catalyst amount = 700 mg, NaOH/glycerol = 2 mol/mol.

in the reaction without heat treatments increases from 4.6 nm (fresh catalyst) to 25 nm after only three runs. Therefore, it seems that the standard procedure for the preparation of catalysts leads to stronger metal/support interactions, slowing down the sinterization rate of Au particles. As the catalyst heat treated at 350 °C presents higher performance and stability, the procedure adopted seems to be the most adequate to prepare the gold catalysts.

The successive experiments carried out with the Au/AC$_0$ catalyst heat treated at 350 °C confirm the influence of the gold dispersion on the catalytic performance, but also allow concluding that even with a metal average size of 11.4 nm (see Table 3) the Au/AC$_0$ catalyst shows a fairly high activity (Fig. 5). Therefore, the poor efficiency of the Au/AC$_1$ catalyst, which has a similar average particle size, cannot be explained only by the gold dispersion.

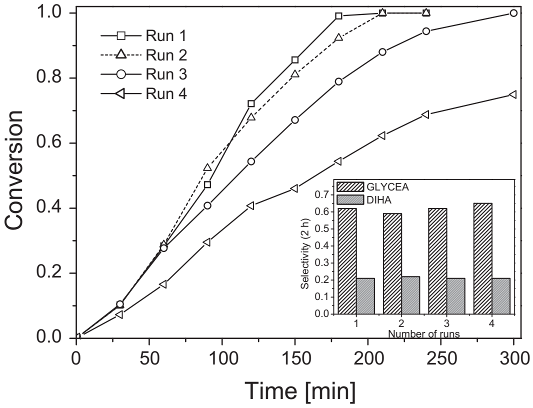

Fig. 5. Successive experiments with the Au/AC$_0$ catalyst. Selectivities to GLYCEA and DIHA at t = 2 h in each cycle are also presented inside. Reaction conditions: 60 °C, p_{O_2} = 3 bar, 150 mL of glycerol 0.3 M, catalyst amount = 700 mg, NaOH/glycerol = 2 mol/mol.

The Au/AC$_1$ catalyst has a high content of oxygenated functional groups and only a residual performance (see Table 2 and Fig. 4). When carboxylic acid groups were removed from the surface (sample Au/AC$_{1tt400}$), no significant enhancement was observed. However, after removing carboxylic acid and carboxylic anhydride groups (sample Au/AC$_{1tt600}$), the catalytic performance improves. Finally, catalysts with a low content of oxygenated surface groups, such as Au/AC$_0$, Au/AC$_{1tt900}$, and Au/AC$_{1tt900-H2}$, show a similar high activity. Therefore, Fig. 4 reveals a strong influence of the surface chemical properties of the support on the catalytic performance in glycerol oxidation, indicating that surface oxygenated groups, mainly those with acid nature, are prejudicial.

As the temperature used in the preparation of supports is increased, oxygenated groups are decomposed sequentially, releasing CO and/or CO_2, and therefore, the resulting supports have a gradual lower amount of oxygen, as it can be seen in Table 2. As a result, the oxygen content of the surface seems to be a factor of large influence in the reaction, since a trend can be observed in Fig. 6. Additionally, TOFs obtained after 2 h of reaction for the different catalysts are also presented in Fig. 6 as a function of the oxygen content. It seems that the catalysts tested can be assorted in three distinct groups:

- Au/AC$_1$ and Au/AC$_{1tt400}$: catalysts with a high amount of oxygen-containing functional groups (mainly acid groups) and low activity.

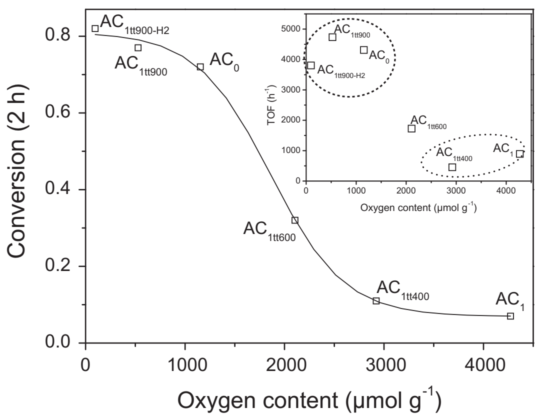

Fig. 6. Influence of the oxygen content of activated carbons on the catalytic performance. *Insert*: TOF after 2 h of reaction for the different catalysts vs. the oxygen content.

- Au/AC_{1tt600}: catalyst with an intermediate amount of oxygen-containing functional groups (lower concentration of acid groups) and intermediate activity.
- Au/AC_0, Au/AC_{1tt900} and $Au/AC_{1tt900\text{-}H2}$: catalysts corresponding to basic supports (only with a limited concentration of oxygenated surface groups, particularly those of acid nature) and high activity.

Summarizing, supports with basic characteristics lead to more active gold catalysts.

Yang et al. [31] tested a series of metal carbonate-supported gold nanoparticles for the liquid-phase oxidation of benzyl alcohol and observed that the catalytic performance depends strongly on the basicity of the support material. They suggest that the initial O-H bond cleavage can occur on the support basic sites. On the contrary, also in a study of benzyl alcohol oxidation, but using activated carbon supports, Zhu et al. [32] concluded that the activity of Au/AC catalysts was improved by the presence of oxygen-containing species on the surface, which were proposed as responsible for oxygen activation.

In Table 6, the selectivities obtained in the presence of the most active catalysts are compared at constant reaction time and at the same glycerol conversion ($X = 40\%$). Contrary to what was observed with the conversions, the presence of oxygenated groups on the support did not influence significantly the selectivities. The prepared catalysts lead to a high total selectivity to products of commercial interest (GLYCEA + DIHA) of about 80%, and a very similar distribution of the products was observed, independently of the amount of oxygenated surface groups present.

3.2.3. Discussion on the influence of support surface chemistry

The role of the support in the catalytic reaction studied is still under discussion. The mechanism for oxygen adsorption and activation on supported gold catalysts is not yet completely established. For the discussion of our observations, it could be assumed that oxygen adsorption proceeds directly on the metal particles [33]. However, in this mechanism, the support would have only a secondary role in the catalytic activity, limited to the dispersion and stabilization of metal particles, and therefore could not explain the results obtained. Additionally, this is not compatible with the well-known low capacity of gold for adsorbing molecular oxygen.

Nevertheless, recent experiments in glycerol oxidation catalyzed by gold supported on carbon showed that oxygen atoms incorporated into the reaction products were originated from hydroxide ions, which play a decisive role during the reaction, and not from molecular oxygen, which is necessary for the

Table 6
Influence of the support on the selectivities of GLYCEA, GLYCOA, DIHA, and TARTA for Au catalysts prepared on activated carbons with different surface chemistries.

Catalyst	$t = 120$ min					$X_{GLY} = 40\%$			
	X_{GLY}	S_{GLYCEA}	S_{GLYCOA}	S_{DIHA}	S_{TARTA}	S_{GLYCEA}	S_{GLYCOA}	S_{DIHA}	S_{TARTA}
Au/AC_0	0.72	0.62	0.15	0.18	0.05	0.59	0.15	0.18	0.04
Au/AC_{1tt600}	0.32	0.64	0.18	0.13	0.05	0.65	0.17	0.13	0.05
Au/AC_{1tt900}	0.78	0.61	0.17	0.13	0.06	0.57	0.20	0.13	0.05
$Au/AC_{1tt900\text{-}H2}$	0.82	0.62	0.15	0.18	0.05	0.61	0.15	0.20	0.04

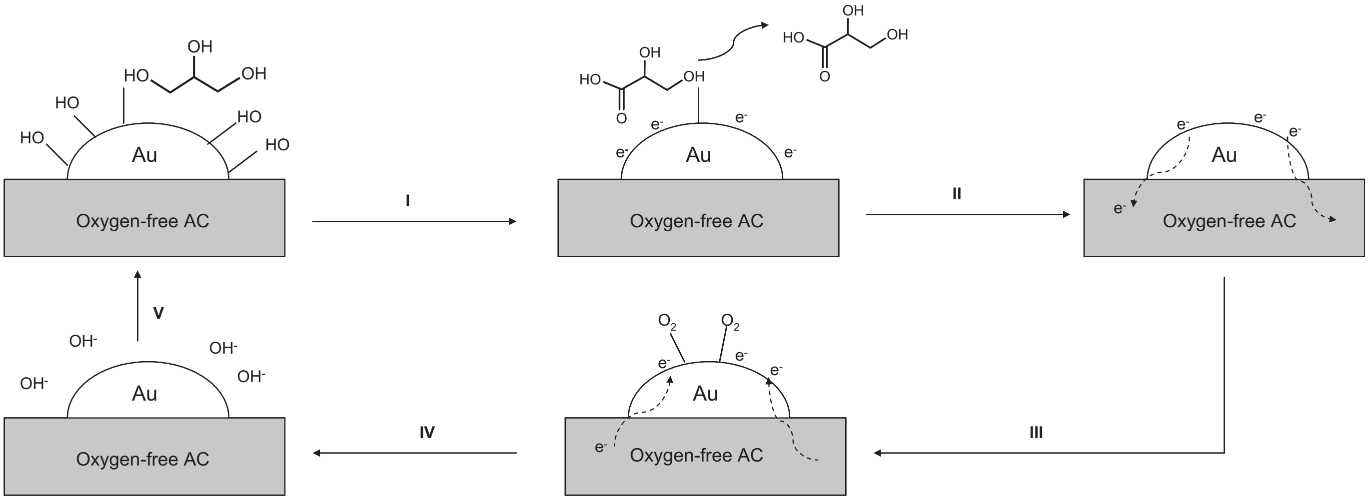

Fig. 7. Role of the basic supports on the mechanism of glycerol oxidation.

regeneration of hydroxide ions [34]. In fact, very poor or no activity is observed when using gold catalysts without a relatively high concentration of added base [24]. Glycerol oxidation is aided by high-pH conditions, since the hydroxide species adsorbed over gold have the ability to facilitate the activation of both the C-H and the O–H bonds of glycerol (also adsorbed on the catalyst surface), leading to the addition of electrons to the metal surface [34] (see Fig. 7; step I). In this way, the oxidation mechanism does not involve the dissociation of molecular oxygen to atomic oxygen. Instead, activation of O_2 occurs by the formation and dissociation of peroxide and hydrogen peroxide intermediates on the metal surface, according to the following mechanism [34]:

$$O_2^* + H_2O^* \rightarrow HOO^* + HO^* \tag{2}$$

$$HOO^* + H_2O^* \rightarrow H_2O_2^* + HO^* \tag{3}$$

$$HO^* + e^- \leftrightarrow HO^- +^* \tag{4}$$

where $*$ represents a site on the metal surface. The last step allows for the removal of electrons added to the surface during the adsorption of hydroxide ions and regenerates these species. In that study [34], the support was not considered to be involved in the mechanism. However, the presence of delocalized π-electrons in basic carbon supports leads to a high electronic mobility, whereas oxygen-containing functional groups (electron-withdrawing groups) decrease the electron density and the electrical conductivity [35,36]. The mobility of electrons to the basic support could potentially reduce the excess of negative charge on gold and enhance the possibility of further hydroxide bonding (Fig. 7, step II), whereas the transition of this electrons from the support to the metal enhance the regeneration of the hydroxide ions (Eqs. (2)–(4) and Fig. 7, steps III and IV). Therefore, the mobility of the electrons from and to the gold surface could potentially promote both adsorption and regeneration of hydroxide ions and thus the catalytic performance.

4. Conclusions

A strong effect of the activated carbon surface chemistry on the activity of Au/AC catalysts for glycerol oxidation was observed. Gold particles with similar average sizes resulted in different performances, depending on the amount of oxygenated groups on the surface of the support used. As a result, the oxygen content on the surface is a factor of large influence in the reaction. Basic oxygen-free supports, characterized by a high density of free π-electrons, lead to an enhancement of the gold catalyst activity. These characteristics can easily be achieved by thermal treatments at high temperatures, which remove the oxygen-containing surface groups. The role of the activated carbon surface chemistry was explained on the basis of a recent published mechanism, by considering the capability of oxygen-free supports to promote electron mobility. The prepared catalysts lead to a high total selectivity to products of commercial interest (GLYCEA + DIHA) of about 80%.

Acknowledgements

This work was carried out with the support of Fundação para a Ciência e a Tecnologia (FCT) under research fellowship BD/45280/2008 (E.G. Rodrigues) and FCT/FEDER in the framework of Program COMPETE (project PTDC/EQU-ERQ/101456/2008). It was also partially supported by Acção Integrada Luso-Espanhola N° E28/11 (Portugal) and Acciones Integradas with reference number AIB2010PT-00377 (Spain). X. Chen acknowledges Ramón y Cajal contract from Ministry of Science and Innovation of Spain.

References

[1] C.H.C. Zhou, J.N. Beltramini, Y.X. Fan, G.Q.M. Lu, Chem. Soc. Rev. 37 (2008) 527.
[2] K. Golz-Berner, L. Zastrow, US Patent 10 570 031, 2007.
[3] P. McMorn, G. Roberts, G.J. Hutchings, Catal. Lett. 63 (1999) 193.
[4] M. Pagliaro, R. Ciriminna, H. Kimura, M. Rossi, C. Della Pina, Angew. Chem. Int. Ed. 46 (2007) 4434.
[5] S. Demirel, K. Lehnert, M. Lucas, P. Claus, Appl. Catal. B 70 (2007).
[6] K. Musialska, E. Finocchio, I. Sobczak, G. Busca, R. Wojcieszak, E. Gaigneaux, M. Ziolek, Appl. Catal. A 384 (2010) 70.
[7] A. Villa, A. Gaiassi, I. Rossetti, C.L. Bianchi, K. van Benthem, G.M. Veith, L. Prati, J. Catal. 275 (2010) 108.
[8] L. Prati, M. Rossi, J. Catal. 176 (1998) 552.
[9] F. Porta, L. Prati, J. Catal. 224 (2004) 397.
[10] G.C. Bond, D.T. Thompson, Catal. Rev. – Sci. Eng. 41 (1999) 319.
[11] W.C. Ketchie, Y.-L. Fang, M.S. Wong, M. Murayama, R.J. Davis, J. Catal. 250 (2007) 94.
[12] F. Porta, L. Prati, M. Rossi, S. Coluccia, G. Martra, Catal. Today 61 (2000) 165.
[13] S. Demirel, P. Kern, M. Lucas, P. Claus, Catal. Today 122 (2007) 292.
[14] E. Papirer, S. Li, J.B. Donnet, Carbon 25 (1987) 243.
[15] J.L. Figueiredo, M.F.R. Pereira, M.M.A. Freitas, J.J.M. Órfão, Carbon 37 (1999) 1379.
[16] J.L. Figueiredo, M.F.R. Pereira, M.M.A. Freitas, J.J.M. Órfão, Ind. Eng. Chem. Res. 46 (2007) 4110.
[17] J.A. Menendez, J. Phillips, B. Xia, L.R. Radovic, Langmuir 12 (1996) 4404.
[18] Y. Onal, S. Schimpf, P. Claus, J. Catal. 223 (2004) 122.
[19] E.G. Rodrigues, S.A.C. Carabineiro, X. Chen, J.J. Delgado, J.L. Figueiredo, M.F.R. Pereira, J.J.M. Órfão, Catal. Lett. 141 (2011) 420.
[20] C.Y. Yin, M.K. Aroua, W.M.A.W. Daud, Sep. Purif. Technol. 52 (2007) 403.
[21] V. Gómez-Serrano, M. Acedo-Ramos, A.J. López-Peinado, C. Valenzuela-Calahorro, Thermochim. Acta 291 (1997) 109.
[22] C. Moreno-Castilla, M.V. Lopez-Ramon, F. Carrasco-Marin, Carbon 38 (2000) 1995.
[23] C.A. Leon y Leon, J.M. Solar, V. Calemma, L.R. Radovic, Carbon 30 (1992) 797.
[24] S. Demirel-Gülen, M. Lucas, P. Claus, Catal. Today 102–103 (2005) 166.
[25] S. Carrettin, P. McMorn, P. Johnston, K. Griffin, C.J. Kiely, G.J. Hutchings, Phys. Chem. Chem. Phys. 5 (2003) 1329.
[26] Y.A. Ryndin, O.S. Alekseev, P.A. Simonov, V.A. Likholobov, J. Mol. Catal. 55 (1989) 109.
[27] S. Carrettin, P. McMorn, P. Johnston, K. Griffin, C.J. Kiely, G.A. Attard, G.J. Hutchings, Top. Catal. 27 (2004) 131.
[28] W.C. Ketchie, M. Murayama, R.J. Davis, J. Catal. 250 (2007) 264.
[29] D. Wang, A. Villa, F. Porta, D. Su, L. Prati, Chem. Commun. (2006) 1956.
[30] N. Dimitratos, J.A. Lopez-Sanchez, D. Lennon, F. Porta, L. Prati, A. Villa, Catal. Lett. 108 (2006) 147.
[31] J. Yang, Y.J. Guan, T. Verhoeven, R. van Santen, C. Li, E.J.M. Hensen, Green Chem. 11 (2009) 322.
[32] J.J. Zhu, S.A.C. Carabineiro, D. Shan, J.L. Faria, Y.J. Zhu, J.L. Figueiredo, J. Catal. 274 (2010) 207.
[33] H.H. Kung, M.C. Kung, C.K. Costello, J. Catal. 216 (2003) 425.
[34] B.N. Zope, D.D. Hibbitts, M. Neurock, R.J. Davis, Science 330 (2010) 74.
[35] D. Sebastián, I. Suelves, R. Moliner, M.J. Lázaro, Carbon 48 (2010) 4421.
[36] Z. Hashisho, M.J. Rood, S. Barot, J. Bernhard, Carbon 47 (2009) 1814.